Materials Science in Semiconductor Processing 139 (2022) 106354

Contents lists available at ScienceDirect

Materials Science in Semiconductor Processing

journal homepage: www.elsevier.com/locate/mssp

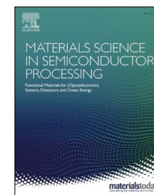

Flexible, solution-processed, indium oxide (In_2O_3) thin film transistors (TFT) and circuits for internet-of-things (IoT)

Sagar R. Bhalerao [a,*], Donald Lupo [a], Paul R. Berger [a,b]

[a] Department of Electrical Engineering, Tampere University, Tampere, Finland
[b] Department of Electrical and Computer Engineering, The Ohio State University, Columbus, USA

ARTICLE INFO

Keywords:
Solution processing
Indium oxide (In_2O_3)
Flexible
Thin film transistor (TFT)
Metal oxide
High-κ gate dielectric
Inverter
Anodization

ABSTRACT

Over the last decade, novel approaches to explore low voltage flexible devices and low power flexible circuits are being widely researched by the scientific community. To realize the true potential of energy thrifty Internet-of-Things (IoT) objects, low power circuits and hence their low-voltage operating devices are a paramount prerequisite, especially when their power is constrained by autonomous energy scavenging. At present, through advanced manufacturing processes, silicon-based semiconductor devices are powering the modern electronics industry. However, processing temperatures are inhibiting them from flexible and printed electronics, as well as being too costly for scalability to the trillions of IoT objects anticipated. Therefore, development of solution-processed metal oxide semiconductors creates huge opportunities for IoT and wearables. Here, flexible solution-processed indium oxide (In_2O_3) thin film transistors (TFT) and inverter circuits with low operating voltage are reported. The operating voltage of the TFTs is ≤ 3 V with threshold voltage (V_{th}) 0.82 V, on/off ratio 10^5 and extracted mobility (μ) in saturation regime is 14.5 $cm^2/V \cdot s$. The gain of the inverter at V_{DD} 1, 2 and 3 V was determined to be 10, 22 and 32 respectively. Furthermore, measured transconductance (g_m) and sub-threshold swing (S) are found to be 140 μS and 0.22 V/dec, respectively.

1. Introduction

Metal oxide semiconductors have gained enormous interest in the design of modern electronics, particularly thin film transistors (TFT), due to their excellent electrical, optical, chemical and mechanical properties. With increasing demand for both high performance and low-voltage operation for low-power consumption, TFTs have been continuously scaled down to their physical limits [1–3]. On the other hand, to achieve low-voltage, high performance TFTs, high-κ dielectrics have been extensively explored for the replacement of silicon oxide. Similarly, tremendous efforts have been devoted to develop solution-processed metal oxide semiconductors for the active channel materials within thin film transistors [4,5]. Additionally, vacuum deposition processes are less scalable to roll-to-roll processing and can concurrently require high processing temperatures [6,7]. Despite dedicated efforts by the research community and industry, there is still only a handful of reports available showing low voltage operating devices with reliable device performance at relatively low temperature processing for semiconductor and high-κ gate dielectric deposition compatible to flexible electronics and Internet-of-Things [8–10]. Moreover, apart from the devices, circuits based on solution processed metal oxide have been given relatively little attention, resulting in a limited number of circuit publications [11–13].

Here, we report the enhanced device performance of flexible thin film transistors (TFTs) based on solution processed indium oxide and comprehensive device bendability study along with SPICE simulations. Furthermore, by utilizing the Transfer Length Measurement (TLM) technique, the contact resistance analysis was provided. In addition to the flexible TFTs, a thorough analysis of a low voltage operating inverter circuit fabricated on a flexible Kapton substrate was also presented.

Solution-processed indium oxide was used as an active semiconductor channel material, which was further combined with a room temperature anodization route to form a thin high-κ aluminum oxide (Al_2O_3) gate dielectric. The room temperature deposition of anodized aluminum oxide carried out as reported previously [14,15], which empowers lower voltage operation i.e. ≤ 3V. The flexible indium oxide TFTs were fabricated by following the bottom gate top contact (BGTC) approach. The schematic representation of the device structure of flexible indium oxide TFTs is shown in Fig. 1(a). Fig. 1(b) illustrates the proposed inverter circuit diagram. A photograph of inverter circuits

* Corresponding author.
E-mail addresses: sagar.bhalerao@tuni.fi (S.R. Bhalerao), pberger@ieee.org (P.R. Berger).

https://doi.org/10.1016/j.mssp.2021.106354
Received 21 August 2021; Received in revised form 7 November 2021; Accepted 23 November 2021
Available online 3 December 2021
1369-8001/© 2021 The Authors. Published by Elsevier Ltd. This is an open access article under the CC BY license (http://creativecommons.org/licenses/by/4.0/).

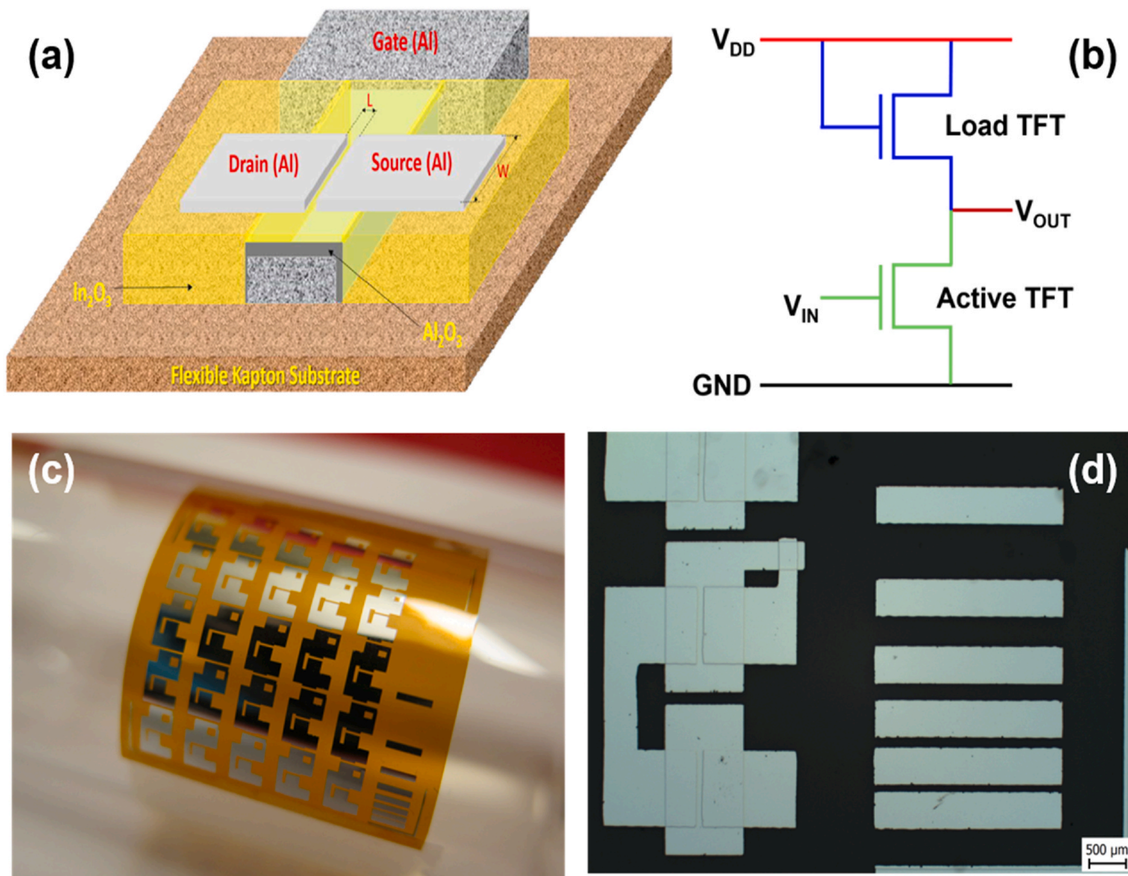

Fig. 1. a) Schematic structure of the In_2O_3 TFT with Al_2O_3 gate dielectric (for illustrative purposes – not on scale). b) Schematic of the proposed inverter circuit. c) A photograph of the fabricated flexible In_2O_3 inverter circuit on a Kapton substrate. and d) Optical micrograph of flexible inverter along with TLM (transfer length measurement) test structure. Scale bar 500 µm.

fabricated on flexible Kapton (Polyimide) is exhibited in Fig. 1(c) and the optical micrograph presented in Fig. 1(d). Additionally, the Transfer Length Measurement (TLM) [16–18] test structure was also fabricated on the same flexible Kapton substrate to investigate the contact resistance along with the electrical performance of the flexible indium oxide TFTs and Inverter circuit.

2. Experimental

As shown in the schematic diagram Fig. 1(a), TFTs were fabricated on a flexible Kapton substrate. Before the fabrication process, the Kapton substrates were thoroughly cleaned with acetone, IPA, and deionized water with subsequent ultrasonication for 30 min. To start with, 100 nm aluminum metal was deposited using a patterned metal shadow mask. Then, anodization process was carried out to form the aluminum oxide gate dielectric. As a result, the top surface of evaporated aluminum metal was transformed into an aluminium oxide (Al_2O_3). The thickness of the subsequent aluminium oxide layer was found to 12 nm thick, which is validated by electron microscopy in our previous report [19]. Following the anodization procedure, the Kapton substrates were rigorously rinsed with deionized water and dried by nitrogen jet to eliminate any residual surface ion impurities from the anodization.

Before applying the active semiconductor channel, a 0.2 M indium oxide solution (ink) was prepared by dissolving Indium (III) nitrate hydrate $In(NO_3)_3{\cdot}xH_2O$ in anhydrous 2-methoxyethanol 99.8%. This prepared solution was further heated at 75 °C for 12 h under continuous stirring prior to spin coating. Subsequently, the indium oxide ink was spun onto the substrate and annealed at 90 °C followed by 300 °C for 15 min and 30 min, respectively, in the air [19]. Finally, again by using a patterned metal shadow mask to form the drain and source contact, 100 nm of Aluminum metal was deposited, forming 1 mm channel width (w) and 80 µm channel length. The same mask also included Transfer Length Measurement (TLM) test patterns to correlate ohmic contact resistance (Fig. 1 (c) and (d)) through varying channel lengths. An e-beam evaporator was used for the aluminum metal deposition, which was performed under a high vacuum 4×10^{-6} Torr. The electrical characterization of the flexible indium oxide TFTs and inverter circuit was performed using a Cascade probe station attached to triaxial shielded probes connected to a Keysight B1500A semiconductor device parameter analyzer.

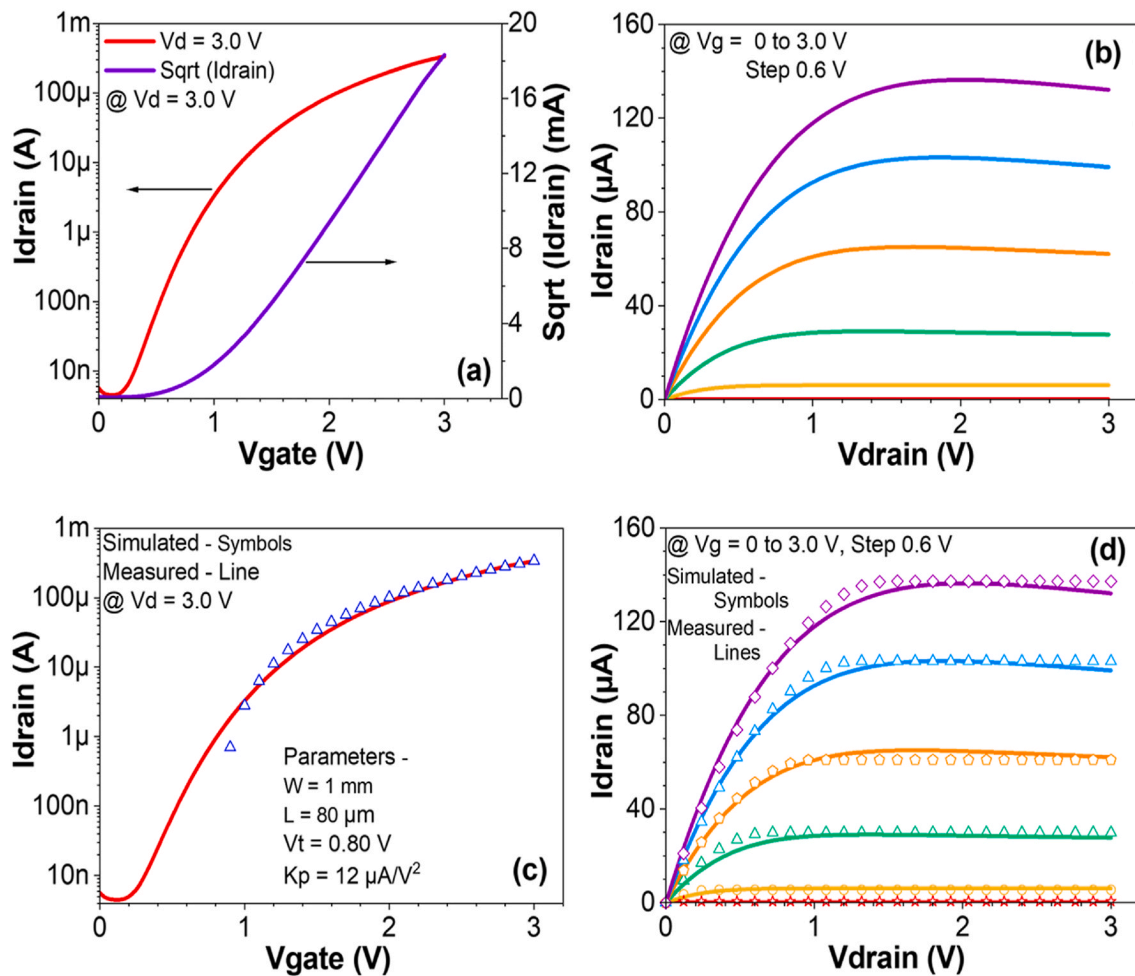

Fig. 2. a) Measured transfer characteristics of flexible In_2O_3 TFTs. b) Measured output characteristics of In_2O_3 TFTs, c) Fitting of a simulation data with a measured transfer characteristic of flexible In_2O_3 TFTs and d) Fitting of a simulation data with a measured output characteristic of flexible In_2O_3 TFTs.

Table 1
Summarized Flexible Indium Oxide TFT performance parameters.

Threshold Voltage (V_{th}) V	Mobility (μ_{sat}) $cm^2V^{-1}s^{-1}$	Transconductance (g_m) μS	Subthreshold swing (S) V/dec
0.82	14.5	140	0.22 V/dec

3. Results and discussion

The measured electrical performance of the flexible indium oxide TFT is shown in Fig. 2 - illustrating transfer characteristics in Fig. 2 (a) and output characteristics in Fig. 2 (b) respectively. Fig. 2 (c) and (d) shows the fitting of the SPICE simulation results superimposed with measured TFTs electrical performance.

The measured and simulated data fitting closely follow one another. The device simulations were performed using the analog devices LTspice software, with physical and measured device parameters, W = 1 mm, L = 80 μm, V_t = 0.82 V and K_p = 12 μA/V^2, which is calculated from equation (1),

$$K_p = \left(\frac{\sqrt{2.I_{d1}} - \sqrt{2.I_{d2}}}{V_{g1} - V_{g2}}\right)^2 \quad (1)$$

where, I_{d1} and I_{d2} are the drain currents at gate voltages V_{g1} and V_{g2}, respectively.

The electrical performance of the flexible TFT conclusively demonstrates low-voltage operation, i.e., functioning at less than 3 V, as well as a significantly lower threshold voltage (V_{th}) is 0.82 V. The flexible TFT exhibited relatively high on/off ratio, 10^5, and the best extracted mobility (μ) was found to be as high as 14.5 cm^2/V·s in saturation regime, which is much higher than previously reported solution-processed, low temperature indium oxide TFTs [20–23]. The electron mobility was calculated using equation (2),

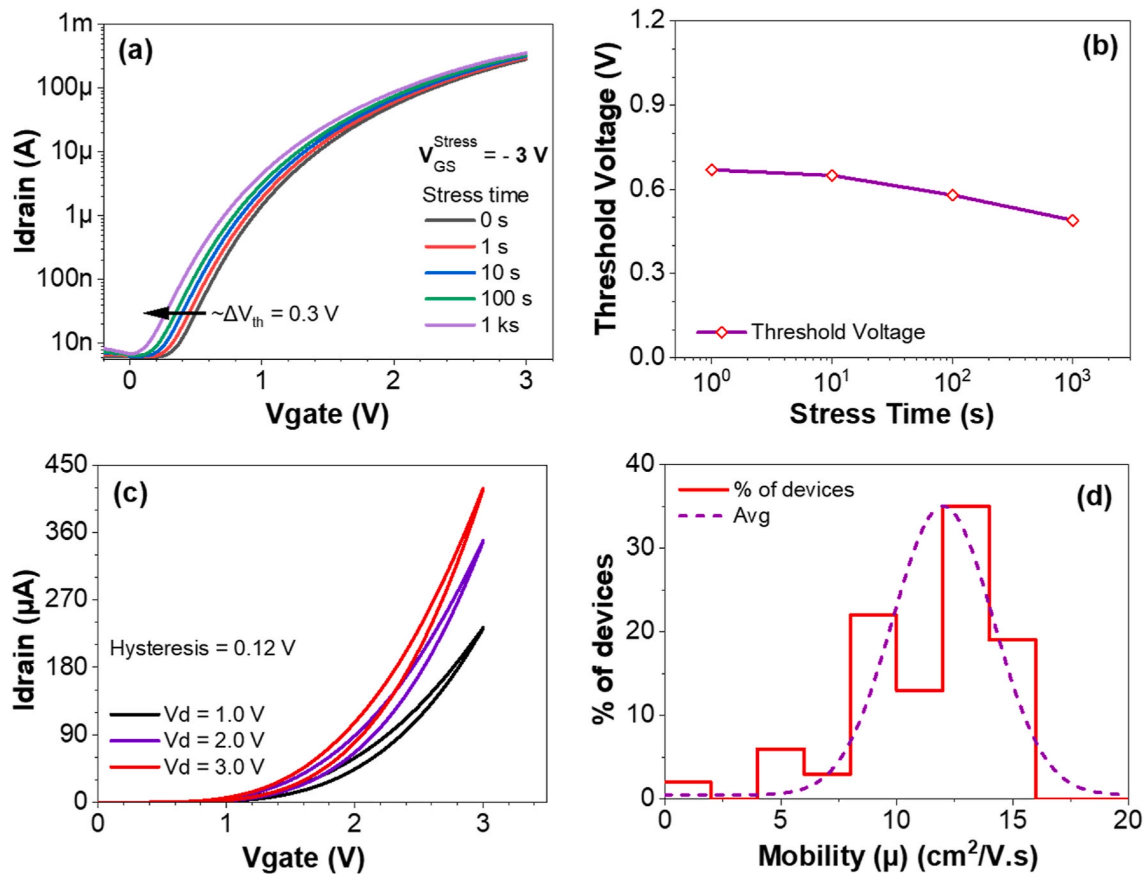

Fig. 3. a) Variation of transfer characteristics (I_d vs. V_g) of In_2O_3 TFTs measured as a function of gate bias stress time, at negative gate bias stress (NBS) of – 3 V, b) Bias stress-induced threshold voltage shift as a function of stress time. During bias stress, a constant gate-source voltage of −3 V was applied, c) Transfer characteristics (I_d vs. V_g) of In_2O_3 TFTs representing negligible hysteresis, and d) The mobility histogram indicating device reliability and yield.

$$\mu_{(sat)} = \frac{\left(\frac{\partial\left(\sqrt{I_D}\right)}{\partial V_G}\right)^2}{\frac{1}{2} C_G \frac{W}{L}} \tag{2}$$

where, I_D is the drain current, V_G is the gate voltage, C_G is the gate oxide capacitance, and W/L is the ratio of width to length of the TFT channel.

From the electrical measurements shown in Fig. 2 (a), the transconductance and subthreshold swing (S) values were also calculated and found to be 140 μS and 0.225 V/dec, respectively. From the Transfer Length Measurement (TLM) shown in Fig. 1 (d), the specific contact resistance (ρ_c) between the metal oxide semiconductor and the metal contacts, i.e. in this case indium oxide and aluminium electrodes, was also measured and was determined to be ~ 0.98 kΩ cm^2. Table 1, summarizes the electrical performance parameters of flexible thin film transistors (TFTs) based on solution processed indium oxide (In_2O_3).

To further investigate device potency, the stability of indium oxide (In_2O_3) TFTs was investigated under bias stress and hysteresis (double scan). Fig. 3 (a) illustrations the transfer characteristics (I_d vs. V_g) of indium oxide TFTs measured at various gate bias stress intervals. Under bias stress, the device performs excellently; nevertheless, a slight shift (negative) in threshold voltage around $\Delta V_{th} = 0.3$ V has been observed, as seen in Fig. 3 (b). It's very likely that this is attributable to joule heating. Furthermore, the indium oxide TFTs' dual-scan transfer characteristics, as shown in Fig. 3 (c), exhibit hysteresis values as low as 0.12 V. Fig. 3 (d) depicts a statistical analysis of the electrical performance of the measured devices as a histogram of saturation mobility versus devices proportion and average, demonstrating that approximately 70% of devices exhibit mobility in the 10–14 cm^2/V·s range, implying excellent device reliability and yield.

We have also studied the bending performance of the indium oxide TFTs with bending radius ranging from 3.5 cm to 5 mm. The specimens were bent around rods of known diameters and measured in the probe station while bent. The variation in mobility as a function of curvature bending is shown in Fig. 4 (a). From the measurements, it was found that there was a slight change in mobility values, ranging from 14.5 to 13.2, over the measurements of bending curvature with radius 3.5 cm to 5 mm. The results are a strong affirmation of the bending stability of this TFT platform technology for wearables [24,25]. The slight change in mobility observed might be attributed from the device handling and/or differences in probing the devices after each bending modification.

Additionally, the electrical performance of the flexible inverter

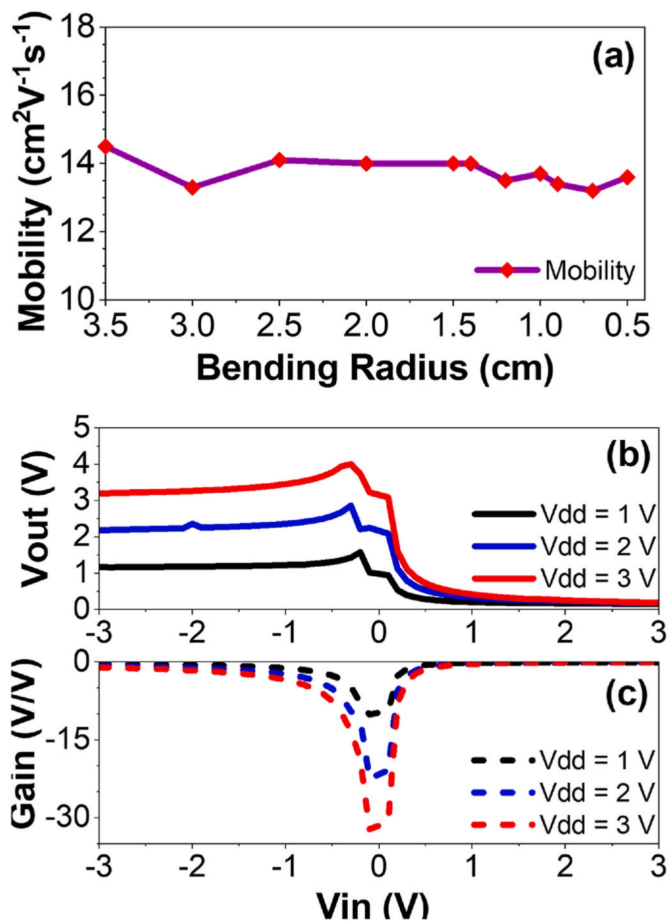

Fig. 4. a) Bending performance of the indium oxide TFTs, b) Voltage transfer characteristics of the flexible solution processed indium oxide inverter at different bias voltage and c) The gain of the flexible inverter circuit.

circuit fabricated based on the solution-processed indium oxide TFTs was also investigated. The voltage transfer characteristics of the indium oxide TFT based inverter circuit (shown in Fig. 1 (b)) at changing supply voltage (V_{DD}) are represented in Fig. 4 (b). From the electrical measurements shown in Fig. 4 (c), the gain of the inverter at V_{DD} was measured in 1 V increments equal to 1, 2 and 3 V and was found to be 10, 22 and 32 respectively.

4. Conclusion

In this work, we successfully demonstrated low voltage, flexible TFTs and inverter circuits based on solution processed indium oxide on the flexible Kapton substrates along with device simulation results. The room temperature anodized high-κ gate dielectric i.e., aluminum oxide enabled the lower device operating voltage below 3 V. The flexible indium oxide TFTs showed excellent electrical performance with electron mobility (μ) as high as 14.5 cm^2/V.s which is significantly higher in terms of state-of-the-art solution-processed, low temperature and low-voltage operating devices. Along with the electrical characteristics, bending performance of the flexible TFTs and inverter circuit also shows stable device performance. The inverter circuit also shows good operating performance over a full scale of input voltage and relatively high gain as high as 32. Therefore, herein not only the device, but also the inverter circuit on a flexible substrate (Kapton Polyimide) has been successfully investigated. Therefore, to envision the true potential of the energy thrifty Internet-of-Things (IoT), low power circuits and hence the low voltage wearables. This study presents, an alternative to the silicon-based semiconductor devices and subsequently, a way forward for flexible, printed electronics and the Internet-of-Things (IoT).

CRediT authorship contribution statement

Sagar R. Bhalerao: Conceptualization, Methodology, Formal analysis, Investigation, Data curation, Writing – original draft, Visualization, Writing – review & editing. **Donald Lupo:** Conceptualization, Resources, Writing – review & editing, Supervision, Project administration, Funding acquisition. **Paul R. Berger:** Conceptualization, Resources, Writing – review & editing, Supervision, Project administration, Funding acquisition.

Declaration of competing interest

The authors declare that they have no known competing financial interests or personal relationships that could have appeared to influence the work reported in this paper.

Acknowledgements

The authors would like to extend a special thanks to Business Finland (Grant no. - 40146/14) and the Academy of Finland for their financial assistance.

References

[1] X. Yu, T.J. Marks, A. Facchetti, Metal oxides for optoelectronic applications, Nat. Mater. 15 (2016) 383–396, https://doi.org/10.1038/nmat4599.
[2] A.D. Franklin, Nanomaterials in transistors: from high-performance to thin-film applications, Science 349 (2015) 6249, https://doi.org/10.1126/science.aab2750.
[3] B. Bayraktaroglu, K. Leedy, R. Neidhard, Microwave ZnO thin-film transistors, IEEE Electron. Device Lett. 29 (2008) 9, https://doi.org/10.1109/LED.2008.2001635.
[4] E. Fortunato, P. Barquinha, R. Martins, Oxide semiconductor thin-film transistors: a review of recent advances, Adv. Mater. 24 (2012) 2945–2986, https://doi.org/10.1002/adma.201103228.
[5] K. Nomura, H. Ohta, A. Takagi, T. Kamiya, M. Hirano, H. Hosono, Room-temperature fabrication of transparent flexible thin-film transistors using amorphous oxide semiconductors, Nature 432 (2004) 488–492, https://doi.org/10.1038/nature03090.
[6] Sangeon Jeon, Jaewan Cho, Sung Min Cho, Photolithography-free fabrication of a-IGZO thin film transistor with interconnecting metal lines, Mater. Sci. Semicond. Process. 121 (2021), 105417, https://doi.org/10.1016/j.mssp.2020.105417.
[7] N. Tiwari, A. Nirmal, M.R. Kulkarni, R.A. John, N. Mathews, Enabling high performance n-type metal oxide semiconductors at low temperatures for thin film transistors, Inorg. Chem. Front. 7 (2020) 1822–1844, https://doi.org/10.1039/d0qi00038h.
[8] J.W. Park, B.H. Kang, H.J. Kim, A review of low-temperature solution-processed metal oxide thin-film transistors for flexible electronics, Adv. Funct. Mater. 30 (2020), 1904632, https://doi.org/10.1002/adfm.201904632.
[9] M.T. Ghoneim, M.M. Hussain, Review on physically flexible nonvolatile memory for Internet of everything electronics, Electronics 4 (2015) 424–479, https://doi.org/10.3390/electronics4030424.
[10] M.R. Shijeesh, A.C. Saritha, M.K. Jayaraj, Investigations on the reasons for degradation of zinc tin oxide thin film transistor on exposure to air, Mater. Sci. Semicond. Process. 74 (2018) 116–121, https://doi.org/10.1016/j.mssp.2017.10.015.
[11] S.R. Bhalerao, D. Lupo, P.R. Berger, 2-volt solution-processed, indium oxide (In_2O_3) thin film transistors on flexible Kapton, IEEE Int. Flexible Electr. Technol. Confer. IFETC (2019) 1–3, https://doi.org/10.1109/IFETC46817.2019.9073721.
[12] K.K. Banger, Y. Yamashita, K. Mori, R.L. Peterson, T. Leedham, J. Rickard, H. Sirringhaus, Low-temperature, high-performance solution-processed metal oxide thin-film transistors formed by a 'sol–gel on chip' process, Nat. Mater. 10 (2011) 45–50, https://doi.org/10.1038/nmat2914.
[13] H. Sirringhaus, T. Kawase, R.H. Friend, T. Shimoda, M. Inbasekaran, W. Wu, E. P. Woo, High-resolution inkjet printing of all-polymer transistor circuits, Science 290 (2000) 2123–2126, https://doi.org/10.1126/science.290.5499.2123.
[14] M. Kaltenbrunner, P. Stadler, R. Schwödiauer, A.W. Hassel, N.S. Sariciftci, S. Bauer, Anodized aluminum oxide thin films for room temperature processed, flexible, low voltage organic non volatile memory elements with excellent charge retention, Adv. Mater. 23 (2011) 4892–4896, https://doi.org/10.1002/adma.201103189.
[15] S.R. Bhalerao, D. Lupo, P.R. Berger, Flexible, gallium oxide (Ga_2O_3) thin film transistors (TFTs) and circuits for the Internet of things (IoT), in: IEEE International Flexible Electronics Technology Conference – IFETC, 2021, pp. 32–34, https://doi.org/10.1109/IFETC49530.2021.9580524.
[16] K.-C. Huang, D.B. Janes, K.J. Webb, M.R. Melloch, A transfer length model for contact resistance of two-layer systems with arbitrary interlayer coupling under the

contacts, IEEE Trans. Electron. Dev. 43 (1996) 676–684, https://doi.org/10.1109/16.491242.
[17] L.W. Guo, W. Lu, B.R. Bennett, J.B. Boos, J.A.d. Alamo, Ultralow resistance ohmic contacts for p-channel InGaSb field-effect transistors, IEEE Electron. Device Lett. 36 (2015) 546–548, https://doi.org/10.1109/LED.2015.2421337.
[18] N. Stavitski, M.J.H. van Dal, A. Lauwers, C. Vrancken, A.Y. Kovalgin, R.A. M. Wolters, Systematic TLM measurements of NiSi and PtSi specific contact resistance to n- and p-type Si in a broad doping range, IEEE Electron. Device Lett. 29 (2008) 378–381, https://doi.org/10.1109/LED.2008.917934.
[19] S.R. Bhalerao, Donald Lupo, Amirali Zangiabadi, Ioannis Kymissis, Jaakko Leppaniemi, Ari Alastalo, Paul R. Berger, 0.6V threshold voltage thin film transistors with solution processable indium oxide (In_2O_3) channel and anodized high-κ Al_2O_3 dielectric, IEEE Electron. Device Lett. 40 (2019) 1112–1115, https://doi.org/10.1109/LED.2019.2918492.
[20] I. Abdullah1, J.E. Macdonald, Y.-H. Lin, T. D Anthopoulos, N.H. Salahr, S.A. Kakil, F. F Muhammadsharif, Bias stability of solution-processed In_2O_3 thin film transistors, J. Phys. Mater. 4 (2021), 015003, https://doi.org/10.1088/2515-7639/abc608.
[21] Y. Zhou, J. Li, Y. Yang, Q. Chen, J. Zhang, Artificial synapse emulated through fully aqueous solution processed low-voltage In_2O_3 thin-film transistor with Gd_2O_3 solid electrolyte, ACS Appl. Mater. Interfaces 12 (2020) 980–988, https://doi.org/10.1021/acsami.9b14456.
[22] D. Khim, Y.-H. Lin, T.D. Anthopoulos, Impact of layer configuration and doping on electron transport and bias stability in heterojunction and superlattice metal oxide transistors, Adv. Funct. Mater. 29 (2019), 1902591, https://doi.org/10.1002/adfm.201902591.
[23] B.S. Kim, H.J. Kim, Influence of annealing on solution-processed indium oxide thin-film transistors under ambient air and wet conditions, IEEE Trans. Electron. Dev. 63 (2016) 3558–3561, https://doi.org/10.1109/TED.2016.2591622.
[24] S.R. Bhalerao, D. Lupo, P.R. Berger, Flexible thin film transistor (TFT) and circuits for Internet of things (IoT) based on solution processed indium gallium zinc oxide (IGZO), in: IEEE International Flexible Electronics Technology Conference – IFETC, 2021, pp. 23–25, https://doi.org/10.1109/IFETC49530.2021.9580506.
[25] P.R. Berger, M. Li, R.M. Mattei, M.A. Niang, N. Talisa, M. Tripepi, B. Harris, S. R. Bhalerao, E.A. Chowdhury, C.H. Winter, D. Lupo, Advancements in Solution Processable Devices Using Metal Oxides for Printed Internet-Of-Things Objects, Electron Devices Technology and Manufacturing Conference, EDTM), 2019, pp. 160–162, https://doi.org/10.1109/EDTM.2019.8731322.